Plant Physiology Preview. Published on June 4, 2012, as DOI:10.1104/pp.112.198424

Running head: Consequences of induced carbon starvation

Journal research area: Whole plant and ecophysiology

Corresponding Author: William R.L. Anderegg, Gilbert Building, Room 109, 371 Serra Mall, Stanford, CA 94305-5020, USA. Phone: (970) 739-4954. Email: anderegg@stanford.edu

Infestation and hydraulic consequences of induced carbon starvation

William R.L. Anderegg[1,2*] and Elizabeth S. Callaway[3]

[1]Department of Biology, Gilbert Building, Room 109, 371 Serra Mall, Stanford University, Stanford CA 94305, [2] Department of Global Ecology, Carnegie Institution for Science, Stanford CA 94305, [3]University of California – Santa Barbara, Santa Barbara CA 94650

Footnotes

Funding for study: Bill Lane Center for the American West, Morrison Institute of Population and Resource Studies, Phi Beta Kappa Northern California Association, Stanford Biology SCORE Program, and Jasper Ridge Biological Preserve. W.R.L.A. was supported in part by an award from the Department of Energy (DOE) Office of Science Graduate Fellowship Program (DOE SCGF). The DOE SCGF Program was made possible in part by the American Recovery and Reinvestment Act of 2009. The DOE SCGF program is administered by the Oak Ridge Institute for Science and Education for the DOE. ORISE is managed by Oak Ridge Associated Universities (ORAU) under DOE contract number DE-AC05-06OR23100. All opinions expressed in this paper are the author's and do not necessarily reflect the policies and views of DOE, ORAU, or ORISE.

Experiment station or institution paper number: N/A

Corresponding author: William R. L. Anderegg, anderegg@stanford.edu

Abstract

Drought impacts on forests, including widespread die-off, are likely to increase with future climate change, though the physiological responses of trees to lethal drought are poorly understood. In particular, *in situ* examination of carbon starvation and its interactions with and effects on infestation and hydraulic vulnerability are largely lacking. In this study, we conducted a controlled, *in situ* repeated defoliation experiment to induce carbon stress in isolated trembling aspen (*Populus tremuloides*) ramets. We monitored leaf morphology, leaves per branch, and multi-tissue carbohydrate concentrations during canopy defoliation. We examined subsequent effects of defoliation and defoliation-induced carbon stress on vulnerability to insect/fungus infestation and hydraulic vulnerability the following year. Defoliated ramets flushed multiple canopies, which coincided with moderate drawdown of non-structural carbohydrate reserves. Infestation frequency greatly increased and hydraulic conductivity decreased one year after defoliation. Despite incomplete carbohydrate drawdown from defoliation and relatively rapid carbohydrate recovery, suggesting considerable carbohydrate reserves in aspen, defoliation-induced carbon stress held significant consequences for vulnerability to mortality agents and hydraulic performance. Our results indicate that multiyear consequences of drought via feedbacks are likely important for understanding forests' response to drought and climate change over the coming decades.

Text

Introduction

Climate change is predicted to have far-reaching effects on the world's forested ecosystems, which cover about 30% of the planet's land surface and store over 45% of Earth's terrestrial ecosystem carbon (Sabine et al. 2004; Bonan 2008). Widespread forest mortality related to drought and temperature stress has already been documented on all six plant-covered continents (Allen et al. 2010). In the western United States, massive tree mortality events have been observed recently across both deciduous and conifer tree species. Several of these events have been linked to severe drought exacerbated by high temperatures, termed "climate change-type droughts" (Logan et al. 2003; Breshears et al. 2005; Allen et al. 2010). Forest mortality events can radically transform regional landscapes and affect ecosystem function, land-atmosphere interactions, carbon sequestration, and ecosystem services provided to humans (Dale et al. 2000; Fischlin et al. 2007; Kurz et al. 2008).

While severe droughts are projected to increase in frequency and intensity with climate change (Fischlin et al. 2007), especially in the southwestern United States (Seager et al. 2007), we currently lack understanding of how forests are likely to respond to drought, including pathways leading to mortality (McDowell et al. 2008; Allen et al. 2010). One prominent proposal is that some forest species may be vulnerable to 'carbon starvation,' where trees experience negative carbon balance during drought, potentially mediated by phloem impairment, eventually leading to tissue-level starvation and mortality (McDowell et al. 2008; Sala et al. 2010). Other physiological failure pathways have been proposed, including 'hydraulic failure' where drought drives a tree's transpiration rate past a critical threshold whereby excessive xylem cavitation by air interrupts plant water transport from roots to leaves. Recent syntheses highlight that carbon-related and hydraulic-related mortality pathways are fundamentally interrelated in many ways, and their interconnections are largely unexplored (McDowell et al. 2011). For instance, limitation of carbohydrate mobilization, translocation, or transport, could influence carbon starvation (Sala et al. 2010; McDowell 2011), and declines in carbon availability could affect hydraulic capacity or defense against insects or pathogens (McDowell et al. 2011). Thus, understanding the role and consequences of carbon starvation could improve our understanding forests' vulnerability to drought.

Tests of the roles of carbon starvation have been limited to date, especially in field environments (McDowell et al. 2008; Hartmann 2011). A greenhouse experiment of mature pine (*Pinus edulis*) trees subjected to severe drought found temperature-driven elevated respiration levels and earlier mortality, potentially implicating carbon starvation, though carbohydrate reserves were not measured directly (Adams et al. 2009; Sala 2009; Leuzinger et al. 2009). Drought experiments on trembling aspen (*Populus tremuloides*) seedlings created symptoms of carbon limitation but led to increases in root stored carbohydrate reserves (Galvez et al. 2011). In one case, low carbohydrate reserves were associated with mortality in a recent study on Scots pine (*Pinus sylvestris*) (Galiano et al. 2011). Yet the potential for carbon starvation in mature trees and, perhaps more importantly, the consequences of carbon limitation on other elements of physiology as a response to drought remain largely unknown.

Most evidence for carbon limitation during drought has been circumstantial, which highlights the critical need for experimental manipulation of these key physiological processes (Niinemets 2010; McDowell 2011). Experimental defoliation is a well-developed technique to examine carbon limitations in field settings (Li et al. 2002; Körner 2003; Snyder & Williams 2003; Markkola et al 2004; Handa et al. 2005; Landhausser & Lieffers 2011) and trade-offs in allocation to growth versus defense (Jones et al. 2004; Osier & Lindroth 2004; Donaldson et al. 2005). We performed a repeated defoliation experiment of mature trembling aspen (*Populus tremuloides*) ramets with the goal of inducing carbon stress/starvation ("carbon stress" defined here as a combination of source limitation (removal of photosynthetic tissue) and sink enhancement (regrowth of successive canopies) (e.g. Handa et al. 2005)).

Trembling aspen, a clonal tree species, is the most widespread tree species in North America (Peterson and Peterson 1992). Trembling aspen are often severely defoliated at regional scales (e.g. Landhausser & Lieffers 2011) in boreal and temperate regions. Aspen forests also recently experienced a widespread drought-induced die-off, termed sudden aspen decline (SAD) (Worrall et al. 2008; Worrall et al. 2010). This mortality event swept across the western United States and parts of Canada following a "climate change-type" drought from 2000-2003 (Worrall et al. 2008; Worrall et al. 2010; Michaelian et al. 2011), and mortality has continued through 2011. Drought and temperature have been implicated as the primary cause of the widespread mortality in a number of studies (Worrall et al. 2008; Worrall et al. 2010; Rehfeldt et al. 2010; Michaelian et al. 2011; Anderegg et al., 2011). Furthermore, previous research has identified

large drought-driven decreases in carbon uptake in trembling aspen in experimental settings (Galvez et al. 2011; Anderegg, 2012). Thus, aspen forests provide an exceptionally timely and relevant case to examine the consequences of carbon stress in this species, both in light of SAD and frequent defoliator outbreaks. Importantly, we do not test here the role of carbon starvation in drought-induced SAD, which has been done elsewhere (Anderegg et al., 2011), but instead seek to understand the consequences of carbon stress, which may play a role in multi-year feedbacks and pathways to mortality.

We performed successive defoliation to induce carbon stress to ask four primary questions. (1) How do canopy patterns (e.g. leaves per branch across branch height), leaf morphology, and leaf area index change during defoliation-induced carbon stress? (2) How does carbon stress manifest in the non-structural carbohydrate reserves in multiple tissues and over time in defoliated ramets? (3) What are the consequences of defoliation-induced carbon stress on vulnerability to insect attack? (4) What are the hydraulic effects of defoliation-induced carbon stress?

Results

We used repeated defoliation on one plot in a paired-plot design in five aspen clones in the San Juan National Forest, Colorado, USA during summer 2010 (see Materials and Methods). A nearby (<10 km) and similar-elevation weather station to the research sites revealed that 2010 had a relatively dry spring, 90% of average snowpack, and average snowmelt around mid-May. During the summer of 2010, the San Juan National Forest received little measurable rain (<0.5cm) between snowmelt and the onset of monsoonal rains in late July, resulting in a seasonal drought. Following a strong monsoonal influx of rain, water year precipitation was still slightly below average for the region (36.8 cm; 42.2 cm average). Water year precipitation for 2011 was barely below average (41.1 cm; 42.2 cm average) with monsoonal influx in early July.

Canopy characteristics of carbon stress

Defoliated plots flushed three canopies over the summer (natural leaf flush (C1) plus 2 canopies following 100% defoliation of 3 ramets (C2 & C3)). Leaf Area Index declined substantially between the three canopies ($p=0.0004$), though this was largely driven by different factors in the second canopy (C2) versus the third canopy (C3) (Figure 1C). Average leaf area

per leaf declined overall ($p<10^{-6}$) and sharply between the C1 and C2, and much less substantially between C2 and C3(Figure 1A). Conversely, number of leaves per branch declined moderately between C1 and C2, but greatly between C2 and C3 ($p<10^{-4}$) (Figure 1B). None of these patterns differed between high and low branches in the canopy, suggesting little sun-leaf/shade-leaf differences in leaf size. We noted very few instances of whole branch die-back in defoliated ramets' canopies. Average leaf net photosynthesis rates did not differ between first (natural) canopy and second (post-defoliation) canopy (A_{first}: 8.4 +/- 1.2 μmol/m^2s (SD); A_{second}: 8.7 +/- 1.4 μmol/m^2s (SD)), which indicates that re-flushed leaves functioned largely as well for carbon uptake as the initial leaves.

In contrast, ramets undergoing Sudden Aspen Decline exhibited strongly directional patterns in canopy die-back. These ramets had much higher rates of mortality in the top and south-sides of the canopy (Figure 2). Our observations of ramets at different stages of canopy dieback suggest that canopy dieback during aspen decline generally starts on high and south-facing branches and proceeds downward and northward.

Carbohydrate dynamics and changes

At no point did carbohydrate concentrations in control ramets differ significantly from native control (un-trenched) ramets, suggesting root-trenching had little effect on carbohydrate balance. Thus, we present here only carbohydrate data of trenched-control and defoliated plots. No carbohydrate concentrations differed between control, defoliated, and native treatments prior to the onset of the experiment. Additionally, no substantial changes were observed in tissue glucose levels, thus only starch and sucrose concentrations are presented here.

Branch starch concentration changed significantly over time ($p<10^{-5}$), between treatments ($p<10^{-3}$), and differently between treatments over time (time-treatment interaction; $p<10^{-4}$) (Figure 3). In contrast, bole xylem starch levels changed significantly over time (p=0.003), though not between treatments or time-treatment interactions (p=0.45, p=0.66). Bole bark starch concentrations changed significantly between treatments, and these differences varied over time (p-treatment=0.013; p-time x treatment interaction= 0.016). Similarly, starch concentrations in roots changed significantly between treatments (p=0.03) and time-treatment interactions (p=0.003). Thus, repeated defoliation strongly influenced branch and root starch concentrations, moderately influenced bark starches, and had little effect on xylem starches.

Branch sucrose levels exhibited significant differences between treatments, although these differences varied over time (p-treatment=0.002; p-time x treatment interaction=0.01) (Figure 4). Bole xylem sucrose, however, showed significant changes only over time (p=0.02) and bark sucrose showed no significant changes across time, treatment, or the interaction. Root sucrose changed significantly only in the time-treatment interaction (p=0.02). This suggests that repeated defoliation only decreased branch and root sucrose levels. We explore specific canopies and tissue-level changes below.

Canopy 1 (Natural leaf-out): Starch concentrations in branches plummeted following initial leaf-out of ramets (p=0.0007) (Figure 3). This indicates that primary reserves for canopy production in aspens likely come from branches. Bole xylem and bark starches declined significantly as well (p_{xylem}=0.004; $p_{bark}<10^{-5}$), while root starches remained steady or increasing. Sucrose levels in xylem, bark, and roots all decreased slightly (Figure 4).

Canopy 2: Following experimental defoliation, newly flushed leaves did not differ in any respect from previous leaves ($Starch_{new}$: 11.3 % +/- 1.1% (SE); $Sucrose_{new}$: 12.8% +/- 1.4%; $Starch_{previous}$: 11.6 % +/- 1.2% (SE); $Sucrose_{previous}$: 13.5% +/- 1.1%). Branch starch concentrations remained low in defoliated ramets', compared to substantial recovery in control ramets (p=0.02), but did not decline lower (Figure 3). Bark starch concentrations exhibited the same pattern as branches with control plots increasing significantly from defoliated plots (p=0.005). Root starch levels exhibited the largest declines (p=0.003). This suggests that the reserves for a second canopy came largely from roots. Sucrose levels declined in roots, bark, and branches in defoliated ramets, but the declines were not significant after the bonferroni correction (Figure 4).

Canopy 3: Following second experimental defoliation, branch starch concentrations remained significantly lower in defoliated plots (p=0.0007) but did not decrease in C3, while root and bark starches recovered to where they were no longer significantly different from control plots(p_{root}=0.07, p_{bark}=0.052). Branch and root sucrose continued to decline, remaining significantly lower in defoliated plots (p=0.0005), while xylem and bark sucrose largely recovered to control levels.

Next Year (NY): By July of 2011, branch starch concentrations remained significantly lower in defoliated plots than control plots (p=0.002), but had recovered in roots to where

defoliated root starch concentrations exceeded those of control plots (p=0.47; Figure 3). Similar recovery and higher levels was observed in branch and root sucrose levels.

Infestation vulnerability

A year following defoliation, rates of infestation increased substantially in defoliated ramets (Figure 5). Frequency of infestation by Cytospera canker and black canker increased significantly (p=0.004; p=0.04 respectively). Though lower levels of infestation occurred with poplar borer and aspen bark beetle, control ramets experienced no infestation by these agents at all.

Hydraulic vulnerability

Hydraulic conductivity did not differ prior to defoliation in 2010, yet measurements in 2011 indicate large shifts in hydraulic capability. By July 2011, defoliated ramets had significantly lower levels of refilled basal area-specific hydraulic conductivity (p=0.007) (Figure 6). This held true for native (un-refilled conductivity) as well (p=0.003), and thus the treatments had no significant difference in PLC (p=0.15). Vulnerability curves indicated a slight increase in vulnerability (higher levels of PLC at less negative water potentials), but this was not significantly different for any water potential (p>0.17) (Figure 6).

Discussion

We characterize here the patterns of induced carbon stress and evidence for subsequent year consequences of carbon stress in trembling aspen. Defoliation-induced carbon stress led to distinct leaf morphology and distribution in subsequent canopies and the following year. This pattern is characterized by smaller leaf area per leaf with few instances of whole-branch dieback, especially in early stages of carbohydrate drawdown. This pattern has been observed in moderate frost-driven defoliation in aspen as well, though severe frost damage led to patchy second canopies (St. Clair et al. 2009). Later stages reveal large decreases in the number of leaves per branch, and most leaves that were flushed tended to be at the distal ends of branches. This pattern contrasts with the observed branch dieback from SAD, which coincides with areas of the canopy more likely to be water stressed due to decreasing xylem water potentials with height and increasing radiation load. Branch die-back tended to occur abruptly across a whole branch. Aspen has highly “sectored” xylem, and SAD crown dieback patterns align with expected patterns of hydraulic failure from aspen xylem structure (Lu et al. 2010).

Likely due to both decreased photosynthesis (source decrease) and the carbon cost of canopy construction (sink increase), defoliation led to carbohydrate decreases in ramets. The source of carbon reserves for the first, natural canopy (C1) and the subsequent post-defoliation canopies (C2,C3) appear to have varied. Branch carbohydrates appeared to have been drawn down for C1, while root reserves declined for C2. A combination of sources may have been used for C3. This aligns with previous research that has suggested the primary storage reserve of aspen carbohydrates is in the clonal root network (Sheppherd & Smith 1993; Landhausser & Lieffers 2011). Root carbohydrate drawdown has been observed in natural defoliation events in aspen clones as well (Landhausser & Lieffers 2011). It also suggests that the seasonal carbohydrate pattern in these forests may be similar to those of the Northern Rocky Mountains, as carbon to construct a normal canopy was drawn from the branches in Alberta (Landhausser & Lieffers 2003). We scaled root and branch starch concentrations by a tissue's biomass, drawn from our measured root biomass and a previously published branch biomass allometric equation calibrated on the same diameter of trees in Utah (Johnston & Bartos 1977), to generate a rough estimate of total tissue starch reserves. Plot-level branch biomass averaged 11.4 kg/plot, while root biomass averaged 6.8 kg/plot. Thus, the branch starch drawdown associated with constructing canopy C1 was approximately 720 g/plot, while the root drawdown associated with C2 was approximately 250 g/plot. This aligns well with the respective biomass and LAI differences between C1 and C2 (Figure 1).

The generally modest declines in carbohydrate reserves, capability for multiple leaf flushes, and relatively rapid recovery of root starch concentrations all suggest substantial carbohydrate reserves in aspen clones. Several other tree species have been found to store enough carbohydrate reserves for multiple canopies as well, which suggests this could be relatively common in mature trees (Niinemets 2010). Notably, despite substantial remaining carbohydrate reserves, subsequent aspen canopies exhibited smaller leaves, fewer leaves per branch, and lower leaf area. This could imply that either: (1) these carbohydrates were not accessible, (2) another nutrient such as nitrogen was limiting for canopy growth, (3) leaf growth in subsequent canopies was slower, or (4) these ramets maintained carbohydrate reserves over canopy growth. Such carbon allocation could allow deciduous trees such as aspens to maintain ample reserves over winter months to flush a healthy canopy in subsequent years. This allocation may also favor increased defense compound synthesis to protect against subsequent defoliations,

which has been documented in defoliated aspen seedlings (Donaldson et al. 2005). Maintaining substantial root NSC reserves may be especially evolutionarily advantageous for aspens because it could allow maintenance of clonal root networks in the soil for longer amounts of time. For instance, aspen root biomass in stands transitioning to conifer forest via succession have been observed to remain relatively constant, despite large losses in aboveground cover (Shepperd et al. 2001).

Moderate drought did occur during the early part of the 2010 growing season, which is a caveat to our results. While it may have slightly influenced the observed canopy characteristics and regrowth, it seems unlikely to have influenced carbohydrate concentrations, as carbohydrate reserves in native aspen clones did not change notably due the drought (Anderegg, 2012). For the infestation and hydraulic analyses, both control and defoliated plots experienced the same drought conditions in both 2010 and 2011. In fact, moderate drought would be most likely to conservatively bias (e.g. decrease signal) of infestation and hydraulic consequences because defoliated plots experienced less water stress due to sharp decreases in transpiration from lower leaf area and canopy duration (Hart et al. 2000).

The multi-year consequences and feedbacks from carbon stress may particularly relevant for drought-induced forest mortality (Landhausser & Lieffers 2011). Defoliated ramets experienced much higher levels of fungus and insect attacks one year following defoliation, which was not documented one year following drought-induced hydraulic failure in a co-occurring experiment (see Anderegg et al. 2011). This is a correlational relationship; increased infestation could have also been influenced by physical or chemical stress responses from the defoliation itself. This caveat is worth bearing in mind regarding application to drought stress, but would certainly occur with natural insect defoliation events. Yet field observations revealed that the spread and severity of the documented insect attacks, even when they did occur in control ramets, appears to have been more severe in defoliated ramets. Combined with the significantly lower levels of branch starch concentrations in 2011, this suggests that carbon stress may have played an important role in vulnerability to infestation. Many of these mortality agents, notably *Saperda calcarata*, can also damage sapwood xylem and therefore could impair hydraulic function as well.

Defoliation-induced carbon stress appears to have had strong effects on hydraulic performance as well. Defoliated ramets had significantly lower branch conductivities one year

following experimental treatment, likely due to declines in growth and new xylem formation. This also highlights the extent to which trembling aspen relies on recent 1-3 years growth for conducting capability, which has been noted in other studies as well (Sperry et al. 1994). Thus, we hypothesize that carbon stress-induced declines in growth during drought may feedback to increased hydraulic vulnerability to drought in subsequent years. Given the multi-year nature of the "climate change-type" drought from 2000-2003, this could have played a role in SAD and die-off events in other species triggered by the same drought (e.g. Breshears et al. 2005).

The mechanisms through which forests respond to severe drought, especially over multiple years, are poorly understood but important for understanding, projecting, and managing the response of forests to future changes in climate. Studies of the physiological and dynamic processes during stress hold great promise for improving our understanding of tree physiology during drought and informing predictive models. We present a multi-tissue, temporal description of defoliation-induced carbon stress and highlight previously little-considered feedbacks of carbon stress, which could influence forests' vulnerability to drought and climate change in the coming decades.

Materials and Methods

Field sites

We performed our experiments on aspen clones in the San Juan National Forest (SJNF), located in southwestern Colorado, USA (Lowry et al. 2007). The San Juan Mountains experience a summer rainy season that usually begins in July due to an influx of monsoonal air from the Gulf of Mexico and the Gulf of California. Previous studies suggested a mean annual temperature of 3.2 ºC and an average annual precipitation of 428 mm at high elevation weather stations (2660-2710 m), though this varies considerably across elevation (Elliot & Baker, 2004). Aspen forests are found from around 2350-3250 m elevation in this region, co-occurring with ponderosa pine (*Pinus ponderosa*) forests at the lower end and Engelmann spruce (*Picea engelmannii*)/subalpine fir (*Abies lasiocarpa*) forests at the upper end (Worrall et al., 2008) .

Defoliation-induced carbon stress experiment

We performed successive 100% canopy defoliation on isolated parts of mature aspen clones to artificially induce carbon stress. Prior to forest leaf-out in May 2010, we located five

aspen clones at low elevation (<2700 m) and largely southern-facing aspects. These attributes are associated with patterns of aspen mortality in previous studies (Worrall et al. 2008) and are thus likely to be vulnerable stands. In these clones, we isolated from the rest of the clone two sets of three healthy ramets in plots of constant area (10 m^2) via mechanical trenching down to bedrock. In these trenches, we measured the diameter of all lateral roots that crossed the root-trench plane along a 2 m-long stretch to calculate root biomass (as in Worrall et al. 2008). All ramets were 3-5 m in height with diameters between 10-14 cm, and contained few to no known aspen pathogens. The two plots were less than 5 m apart in all clones. These five clones represent the replication unit for all analysis of the study, as one of each paired plot was defoliated and the other plot was a control (see below). In addition, we included a "native stems" control treatment of 3 stems per clone >20 m from the paired plots which received no manipulation of any kind.

For baseline non-structural carbohydrate (NSC) analysis, we sampled a small amount of root, branch (twig), bole sapwood xylem, and bole bark tissues (2-3 cm tissue; N=3 per tissue per plot) within plots and the same tissues (N=3 per tissue per clone) of nearby native ramets for carbohydrate analysis. We sampled coarse roots (diameter 3-6 mm) via careful excavation with a shovel.

Following leaf-out (termed Canopy 1 or C1 henceforth), we sampled the same tissues in plot ramets and native ramets for carbohydrate analysis. Additionally, we marked two branches per ramet (diameter: 3-6 mm), one near the apical leader and one near the lower edge of the canopy, in defoliated ramets. We recorded number of leaves per branch and, post-defoliation, average leaf area per leaf by calculating area of defoliated leaves via ImageJ (ImageJ). We measured the photosynthetic rates of ramet leaves via gas exchange (LI-COR 6400) at ambient humidity and CO_2 with photosynthetically active radiation (PAR) provided by an LED light at 1500 ($\mu mol/m^2s$). We then randomly assigned one of the two plots to be experimentally defoliated to impose carbon stress. We manually defoliated 100% of the three ramets' canopies from ladders (June 12-19), taking exceptional care not to damage any branch tissue and to remove leaves at the petiole. We saved and dried leaves for dry-mass leaf area index calculations.

We noted the dates of leaf-flush and defoliation in each plot, standardizing the length of flush + leaf growth period between plots. Within 10-15 days, defoliated ramets re-flushed leaves (Canopy 2; C2). We allowed the same growth period in each plot as in the first canopy flush. We

sampled all major tissues (leaf, branch, root, bole xylem, and bole bark) for carbohydrate analysis from all three treatments (defoliated, trenched-control, and native-control). We measured leaves per branch and average leaf area per leaf in all ramets. Additionally, we measured photosynthetic performance of the new leaves via gas exchange. Immediately following these measurements, we then defoliated the ramets once more with the same methods (July 15-25). Within 12-17 days, defoliated ramets re-flushed leaves again (Canopy 3; C3). We waited the same amount of time as before and then made final tissue collections and branch measurements, identical to previous sampling methods. We calculated Leaf Area Index per plot at each sampling event by developing an average ratio of leaf area to dry mass (specific leaf area) and then multiplied this ratio by the total leaf dry-mass from each ramet.

Carbohydrate analysis

After excising from the ramet, we kept samples on ice (typically 4-8 hours) for transport to a lab. We then oven-dried all samples at 50 ^{o}C and ground samples in a wiley-mill (30 mesh) and ball-mill. In the case of roots, we combined root samples of each plot (three roots per plot into the same sample) at the ball-mill stage by adding equal weights of each root to the ball-mill, thereby averaging the individual roots. This has been done successfully in previous carbohydrate analysis of aspens (Landhausser & Lieffers 2002; Anderegg et al., 2011) and we ran several analyses with roots separate and combined, which yielded no significant differences (students t-test, $t=0.51$, $p=0.86$). We extracted glucose, sucrose, and starch from all collected tissues. We followed the carbohydrate extraction procedure described in Raab (1995), which involves chloroform extraction of free sugars, enzymatic digestion of sucrose via invertase (Sigma-Aldrich: I9274), and enzymatic digestion of starch via beta-amylase (Sigma-Aldrich: A7130) and amyloglucosidase (Sigma-Aldrich: 10115-1G-F). After sucrose and starch digestion, levels of carbohydrates were measured colormetrically via MBTH dye (3-Methyl-2-benzothiazolinone hydrazone hydrochloride; Sigma-Aldrich: 149022-15-1) at 595 nm.

Observational measures of canopy mortality

As a reference for comparison, we determined the canopy characteristics of dieback from SAD. We estimated canopy mortality in seven clones near the defoliated plots that have a <100 m-long mortality gradient within the same clone from a largely healthy area to a largely dead area (see Anderegg et al. 2011 for full methods). Briefly, clones did not differ significantly in elevation, aspect, hydrology, or stem diameter across the mortality gradient. To ensure we were

working within the same clone (genetically identical ramets) we distinguished adjacent clones by observing leaf-flush and leaf coloration phenology, which occur largely simultaneously across a given clone. We assessed canopy mortality visually in ten ramets per clone as in Worrall et al. (2010). Additionally, we estimated average height of dead branches, and average direction of canopy mortality by using dead branches as references of canopy mortality. To validate these canopy mortality estimates and improve standardization of methods, we compared estimated mortality to Leaf Area Index assessed via fish-eye photography. Our method agreed well (r=0.93) with photographic estimates of leaf area and canopy cover.

Follow up, insect vulnerability, and hydraulic analysis

To determine the multiyear effects of carbon stress, we returned to the defoliated plots in July 2011. We examined changes in tissue carbohydrate concentration, vulnerability to infestation, and hydraulic vulnerability. We collected tissue samples of branches and roots for carbohydrate analysis with the same methods. We noted the presence or absence of pathogen or insect attack of defoliated ramets compared to control ramets for four of the main infestation agents involved with SAD. While no primary mortality agents (pathogens or insects that typically kill healthy ramets) are involved with SAD, 4-6 secondary agents are associated with the decline (Worrall et al. 2010). We measured the frequency of attack of Cytospera canker (*Cytospora chrysosperma*), black canker (*Ceratocystis populicola*), poplar borer (*Saperda calcarata*), and aspen bark beetle (*Trypophloeus populi*) within our plots. We also collected two branches per treatment in each plots for hydraulic analysis. All branches were cut, immediately immersed in water, placed in plastic bags for rapid transport to the lab, and then re-cut under water with a razor blade prior to measurement. We conducted measurements of native conductivity, refilled conductivity, and percent loss of conductivity (PLC) per the pressure-flow method of Sperry et al. (1988). In addition, we quantified a hydraulic 'vulnerability curve,' a standard relationship between branch water potential and PLC, via the air injection technique (Sperry and Saliendra 1994).

Statistical Analyses

We examined the effect of defoliation on carbohydrate reserves in each tissue via repeated-measures ANOVA (within samples: plot over time; treatment: control versus defoliation), testing the assumption of sphericity using Mauchly's Sphericity Test. We further tested differences in average leaf area per leaf, leaves per branch, and leaf area index over time

in the defoliated plots by using a one-way ANOVA (factor: time period). We performed pairwise t-tests on selected means from ANOVAs for post-hoc tests, provided assumptions of sphericity and homogeneity of variances held, correcting for multiple hypothesis testing with a bonferroni correction. All analyses were conducted in R (R-project.org Version 2.12.1).

Acknowledgements

We thank L. Anderegg, M. Anderegg, J. Sprague, E. Sprague, C. Sprague, G. Robinson for assistance with fieldwork. We thank E. Pringle, T. Raab, L. Anderegg, A. Winslow, A. Hausladen, N. Bitler, A. Lunny, W. Lagrandeur, J. Burr, A. Hines, M. Erviti, G. Griffin, M. Dini, S. Shin, K. Belcher, N. Walzebuck, K. Marren, L. Oswald for assistance in laboratory work. We thank H. Mooney, J. Berry, L. Anderegg and C. Field for helpful comments on the manuscript.

References

Adams HD, et al. (2009) Temperature sensitivity of drought-induced tree mortality portends increased regional die-off under global-change-type drought. Proceedings of the National Academy of Sciences **106**:7063-7067

Allen CD, et al. (2010) A global overview of drought and heat-induced tree mortality reveals emerging climate change risks for forests. Forest Ecology and Management **259**:660-684.

Anderegg WRL, et al. (2011) The roles of hydraulic and carbon stress in a widespread climate-induced forest die-off. Proceedings of the National Academy of Sciences. doi:10.1073/pnas.1118276108

Anderegg WRL (2012) Complex aspen forest carbon and root dynamics during drought. Climatic Change **111**: 983-991

Bonan GB (2008) Forests and climate change: forcings, feedbacks, and the climate benefits of forests. Science **320**:1444-1450.

491 Breshears DD, et al. (2005) Regional vegetation die-off in response to global-change-type
492 drought. Proceedings of the National Academy of Sciences **102**:15144-15148.

493 Cox PM, et al. (2004) Amazonian forest dieback under climate-carbon cycle projections for the
494 21st century. Theoretical and Applied Climatology **78**:137-156.

495 Dale VH, Joyce LA, McNulty S, Neilson RP (2000) The interplay between climate change,
496 forests, and disturbances. Science of the Total Environment, The **262**(3):201-204.

497 Donaldson JR, Kruger EL, Lindroth RL (2005) Competition- and resource-mediated tradeoffs
498 between growth and defensive chemistry in trembling aspen (Populus tremuloides). New
499 Phytol **169**: 561-570

500 Elliot GP, Baker WL (2004) Quaking aspen (Populus tremuloides) at treeline: A century of
501 change in the San Juan Mountains, Colorado USA. Journal of Biogeography, **31:** 733-745.

502 Fischlin A, et al. (2007) Ecosystems, their Properties, Goods, and Services, Chapter 4 in: Climate
503 Change 2007: Climate Change Impacts, Adaptation and Vulnerability, The IPCC Fourth
504 Assessment Report. Cambridge University Press, Cambridge, UK.

505 Galiano L, Martinez-Vilalta J., Lloret F (2011) Carbon reserves and canopy defoliation
506 determine the recovery of Scots pine 4 yr after a drought episode. New Phytologist **190**: 750-
507 759.

508 Galvez DA, Landhäusser SM, Tyree MT (2011) Root carbon reserve dynamics in aspen
509 seedlings: does simulated drought induce reserve limitation? Tree Physiology **31**:250–257.

510 Handa IT, Korner C, Hattenschwiler S (2005) A test of the treeline carbon limitation hypothesis
511 by in situ CO_2 enrichment and defoliation. Ecology **86**: 1288-1300

512 Hart M, Hogg EH, Lieffers VJ (2000) Enhanced water relations of residual foliage following
513 defoliation in Populus tremuloides. Can. J. Bot. **78**: 583–590

514 Hartmann H (2011) Will a 385 million year-struggle for light become a struggle for water and
515 for carbon? – How trees may cope with more frequent climate change-type drought events.
516 Global Change Biology, **17**: 642–655.

517 ImageJ. Image processing software < http://rsbweb.nih.gov/ij/index.html> Accessed 1 February,
518 2010.

519 Jones B, Tardif J, Westwood R (2004) Weekly xylem production in trembling aspen (Populus
520 tremuloides) in response to artificial defoliation. Can. J. Bot. **82**: 590–597

521 Keen RA (1996) Weather and climate. In: The Western San Juan Mountains: Their Geology,
522 Ecology, and Human History (in ed Blair R), pp 113-126. University of Colorado Press,
523 Boulder, Colorado.

524 Körner C (2003) Carbon limitation in trees. Journal of Ecology **91**: 4-17

525 Kurz WA, et al. (2008a) Mountain pine beetle and forest carbon feedback to climate change.
526 Nature **452**:987-990.

527 Kurz WA, Stinson G, Rampley GJ, Dymond CC, Neilson ET (2008b) Risk of natural
528 disturbances makes future contribution of Canada's forests to the global carbon cycle highly
529 uncertain. Proceedings of the National Academy of Sciences **105**:1551-1555.

530 Landhausser SM, Lieffers VJ (2003) Leaf area renewal, root retention and carbohydrate reserves
531 in a clonal tree species following above-ground disturbance. Journal of Ecology **90**: 658-666

532 Landhausser SM, Lieffers VJ (2011) Defoliation increases risk of carbon starvation in root
533 systems of mature aspen. Trees DOI 10.1007/s00468-011-0633-z

534 Leuzinger S, Bigler C, Wolf A, Körner C (2009) Poor methodology for predicting large-scale
535 tree die-off. Proceedings of the National Academy of Sciences **106**, E106.

536 Li M, Hoch G, Körner C (2002) Source/sink removal affects mobile carbohydrates in *Pinus*
537 *cembra* at the Swiss treeline. Trees - Structure and Function **16**: 331-337

538 Logan, JA, Regniere L, Powell JA (2003) Assessing the impacts of global warming on forest
539 pest dynamics. Frontiers in Ecology and the Environment **1**:130-137.

540 Lowry J, et al. (2007) Mapping moderate-scale land-cover over very large geographic areas
541 within a collaborative framework: A case study of the Southwest Regional Gap Analysis
542 Project (SWReGAP). Remote Sensing of Environment, **108**: 59-73.

Markkola A, Kuikka K, Rautio P, Härmä E, Roitto M, Tuomi J (2004) Defoliation increases carbon limitation in ectomycorrhizal symbiosis of *Betula pubescens*. Oecologia **140**: 234-240

McDowell N, et al. (2008) Mechanisms of plant survival and mortality during drought: why do some plants survive while others succumb to drought? New Phytologist **178**:719-739.

McDowell N (2011) Mechanisms Linking Drought, Hydraulics, Carbon Metabolism, and Vegetation Mortality. Plant Physiology **155**: 1051-1059

McDowell N, Beerling DJ, Breashers DD, Fisher RA, Raffa RF, Stitt M (2011) The interdependence of mechanisms underlying climate-driven vegetation mortality. Trends in Ecology and Evolution **26**: 523-29

Michaelian M, Hogg EH, Hall RJ, and Arsenault, E (2011) Massive mortality of aspen following severe drought along the southern edge of the Canadian boreal forest. Global Change Biology, **17**: doi: 10.1111/j.1365-2486.2010.02357.x

Narisma GT, et al (2003) The role of biospheric feedbacks in the simulation of the impact of historical land cover change on the Australian January climate. Geophysical Research Letters **30**: 2168-2172.

Niinemets U (2010) Responses of forest trees to single and multiple environmental stresses from seedlings to mature plants: Past stress history, stress interactions, tolerance and acclimation. Forest Ecology and Management. **260**: 1623-1639

Osier TL, Lindroth RL (2004) Long-term effects of defoliation on quaking aspen in relation to genotype and nutrient availability: plant growth, phytochemistry and insect performance. Oecologia **139**: 55–65.

Peterson EB & Peterson NM (1992) Ecology, management, and use of aspen and balsam poplar in the prairie provinces, Canada. Aspen Bibliography:2512.

Raab TK & Terry N (1995) Carbon, nitrogen, and nutrient interactions in Beta vulgaris L. as influenced by nitrogen source, NO3-versus NH4+. Plant physiology **107**:575-590.

568 Rehfeldt GE, Ferguson D, Crookston N. (2009) Aspen, climate, and sudden decline in western
569 USA. Forest ecology and management **258**: 2353-2367.

570 Sala A (2009) Lack of direct evidence for the carbon-starvation hypothesis to explain drought-
571 induced mortality in trees. Proceedings of the National Academy of Sciences **106**:E68.

572 Sabine CL et al. (2004) In The Global Carbon Cycle: Integrating Humans, Climate, and the
573 Natural World, C. B. Field, M. R. Raupach, Eds. Island Press, pp 17–44.

574 Sala A, Piper F, & Hoch G (2010) Physiological mechanisms of drought induced tree mortality
575 are far from being resolved. New Phytologist **186**:274-281.

576 Seager, R, Ting MF, Held I, Kushnir Y, Lu J, Vecchi G, Huang HP, Harnik N, Leetmaa A, Lau
577 NC, Li CH, Velez J, Naik N (2007) Model projections of an imminent transition to a more
578 arid climate in southwestern North America. Science **316**:1181-1184.

579 Shepperd WD, Smith FW (1993) The role of near-surface lateral roots in the life cycle of aspen
580 in the central Rocky Mountains. Forest Ecology and Management **61**: 157–170

581 Shepperd WD, Bartos DL, Mata SA (2001) Above- and below-ground effects of aspen clonal
582 regeneration and succession to conifers, Canadian Journal of Forest Resources **31**: 739–745.

583 St. Clair SB, Monson SD, Smith EA, Cahill DG, Calder WG (2009) Altered leaf morphology,
584 leaf resource dilution and defense chemistry induction in frost-defoliated aspen (Populus
585 tremuloides). Tree Phys **29**: 1259-1268.

586 Snyder KA, Williams DG (2003) Defoliation alters water uptake by deep and shallow roots of
587 *Prosopis velutina* (Velvet Mesquite). Functional Ecology **17**: 363-374

588 Worrall JJ, et al. (2008) Rapid mortality of Populus tremuloides in southwestern Colorado, USA.
589 Forest Ecology and Management **255**:686-696.

590 Worrall et al. (2010) Effects and etiology of sudden aspen decline in southwestern Colorado,
591 USA. Forest ecology and management. **250**: 638-349.

592

Figure Legends

Figure One: Canopy characteristics (Mean +/- SE) of defoliated ramets after first canopy flush (C1), second canopy flush (C2) and third canopy flush (C3). (A) Average area per leaf (cm^2); (B) Average number of leaves per branch; and (C) Leaf Area Index (m^2/m^2).

Figure Two: Distribution of average canopy mortality of Sudden Aspen Decline-affected ramets. Average height of mortality within the canopy (left) and direction of mortality (right).

Figure Three: Starch levels (Mean +/- SE) of branch, xylem, bark, and root tissues in control ramets (white) and defoliated ramets (gray) over the course of the experiment. Sampling events were Pre-Leaf flush (PL), first canopy flush (C1), second canopy flush of defoliated ramets (C2) and third canopy flush of defoliated ramets (C3), and the next year (NY) following defoliation. Note: NY samples were not taken from Xylem/Bark tissues.

Figure Four: Sucrose levels (Mean +/- SE) of branch, xylem, bark, and root tissues in control ramets (white) and defoliated ramets (gray) over the course of the experiment. Sampling events were Pre-Leaf flush (PL), first canopy flush (C1), second canopy flush of defoliated ramets (C2) and third canopy flush of defoliated ramets (C3), and the next year (NY) following defoliation. Note: NY samples were not taken from Xylem/Bark tissues.

Figure Five: Frequency (Mean +/- SE) of fungus or insect attacks in control (white) and defoliated (gray) ramets one year following defoliation for Cytospera canker (*Cytospora chrysosperma*), black canker (*Ceratocystis populicola*), poplar borer (*Saperda calcarata*), and aspen bark beetle (*Trypophloeus populi*).

Figure Six: (A) Refilled basal area-specific hydraulic conductivity (Mean +/- SE; g/mm*kPa*s) in control (white) and defoliated (gray) ramets in 2010 prior to defoliation and in 2011. (B) Percent loss conductivity of control (white) and defoliated (black) ramets as a function of branch water potential.

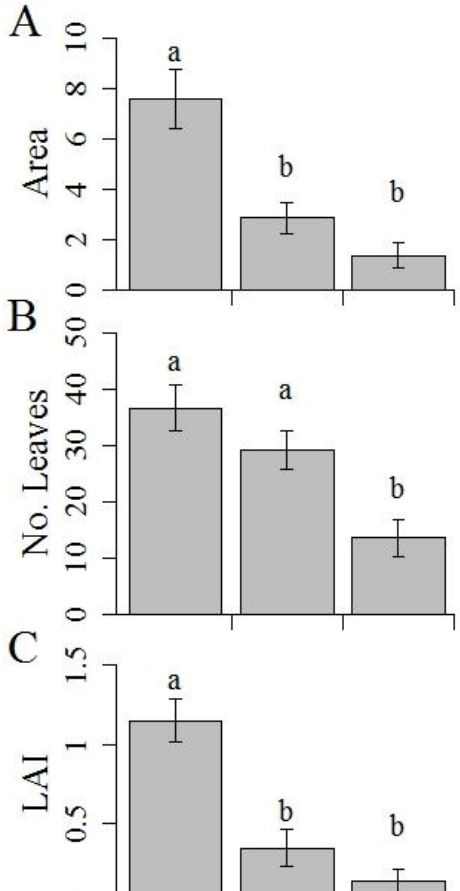

Figure One: Canopy characteristics (Mean +/- SE) of defoliated ramets after first canopy flush (C1), second canopy flush (C2) and third canopy flush (C3). (A) Average area per leaf (cm^2); (B) Average number of leaves per branch; and (C) Leaf Area Index (m^2/m^2).

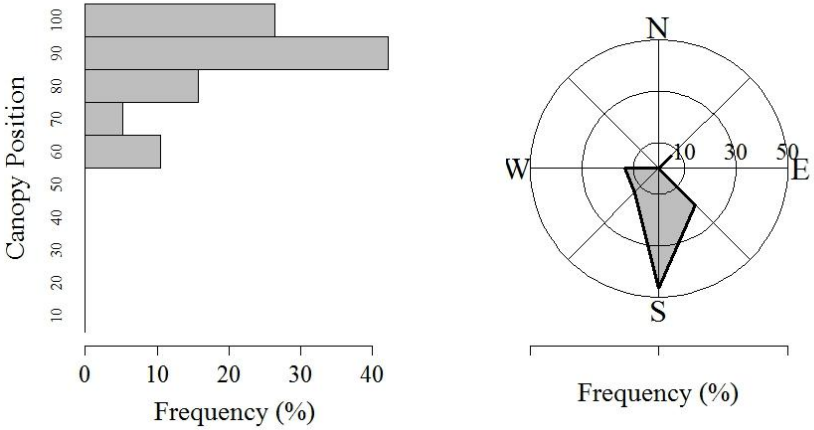

Figure Two: Distribution of average canopy mortality of Sudden Aspen Decline-affected ramets. Average height of mortality within the canopy (left) and direction of mortality (right).

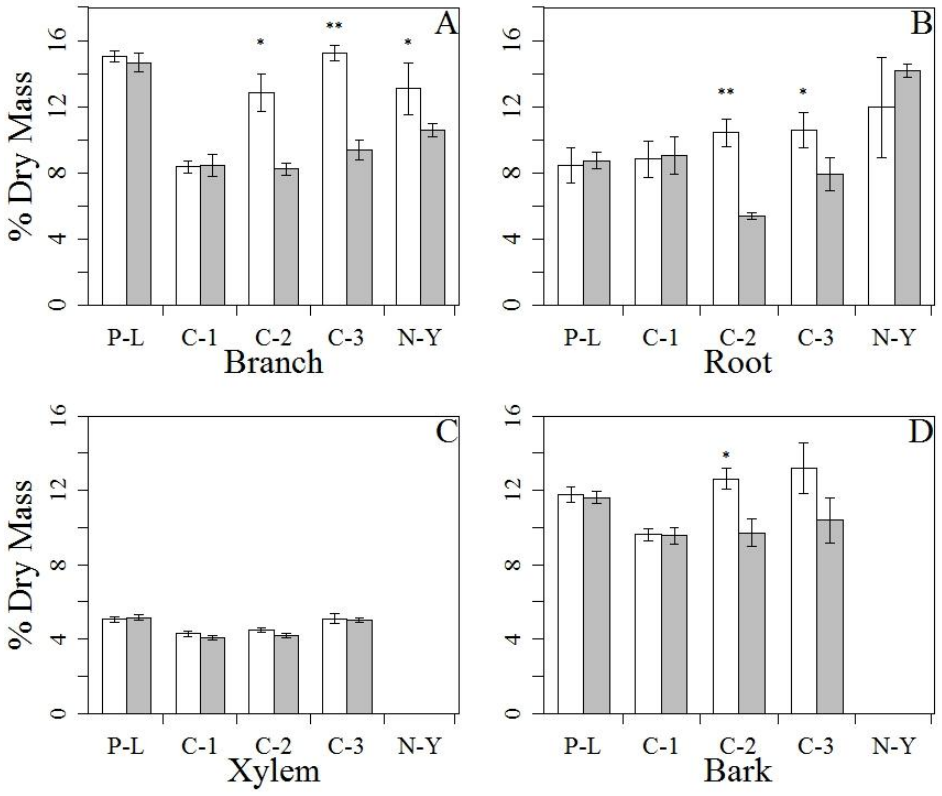

Figure Three: Starch levels (Mean +/- SE) of branch, xylem, bark, and root tissues in control ramets (white) and defoliated ramets (gray) over the course of the experiment. Sampling events were Pre-Leaf flush (PL), first canopy flush (C1), second canopy flush of defoliated ramets (C2) and third canopy flush of defoliated ramets (C3), and the next year (NY) following defoliation. Note: NY samples were not taken from Xylem/Bark tissues.

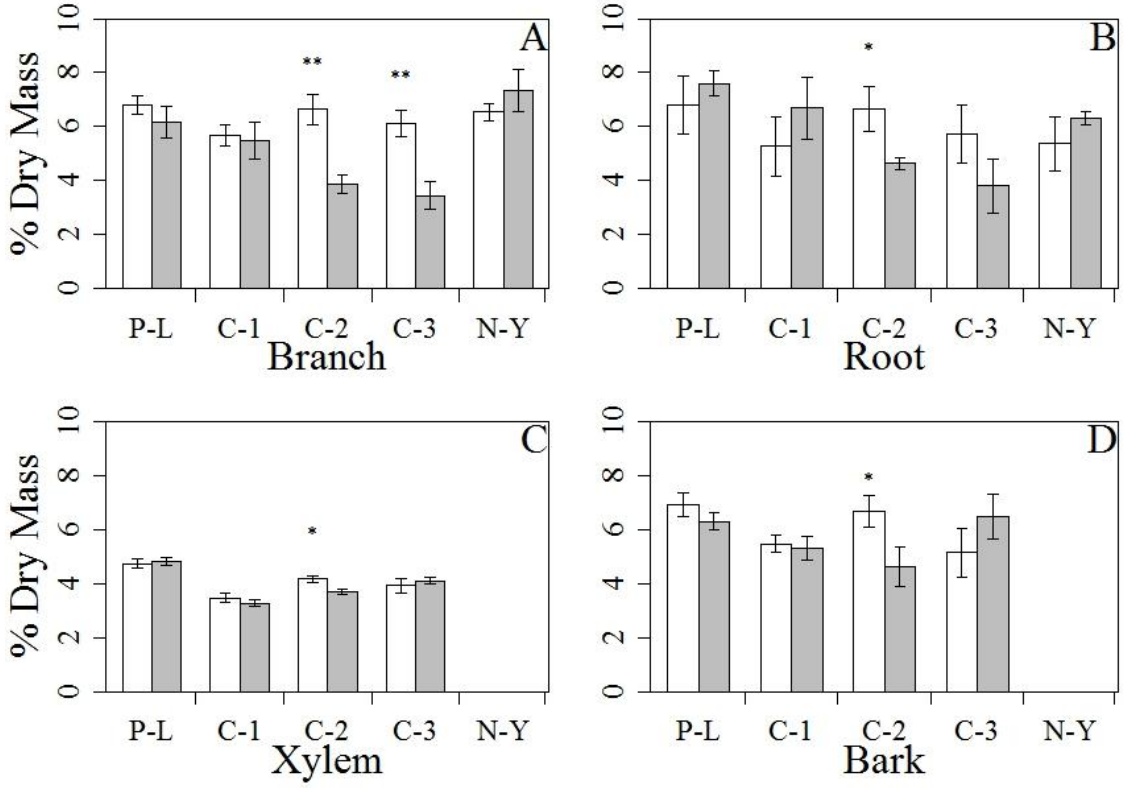

Figure Four: Sucrose levels (Mean +/- SE) of branch, xylem, bark, and root tissues in control ramets (white) and defoliated ramets (gray) over the course of the experiment. Sampling events were Pre-Leaf flush (PL), first canopy flush (C1), second canopy flush of defoliated ramets (C2) and third canopy flush of defoliated ramets (C3), and the next year (NY) following defoliation. Note: NY samples were not taken from Xylem/Bark tissues.

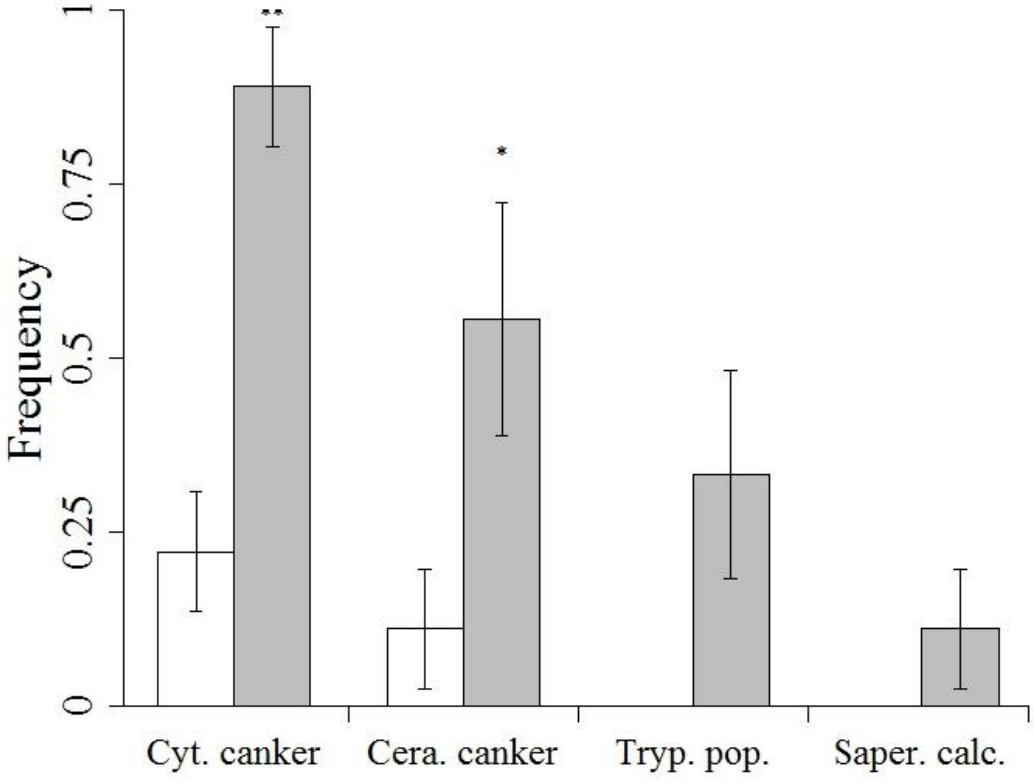

Figure Five: Frequency (Mean +/- SE) of fungus or insect attacks in control (white) and defoliated (gray) ramets one year following defoliation for Cytospera canker (*Cytospora chrysosperma*), black canker (*Ceratocystis populicola*), poplar borer (*Saperda calcarata*), and aspen bark beetle (*Trypophloeus populi*).

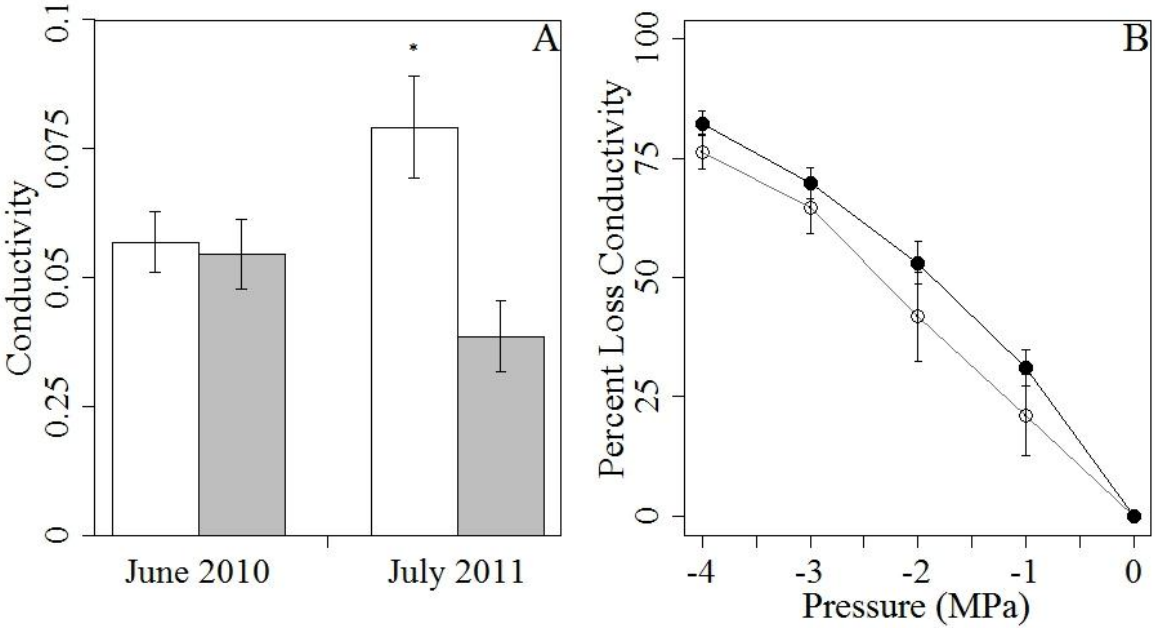

Figure Six: (A) Refilled basal area-specific hydraulic conductivity (Mean +/- SE; g/mm*kPa*s) in control (white) and defoliated (gray) ramets in 2010 prior to defoliation and in 2011. (B) Percent loss conductivity of control (white) and defoliated (black) ramets as a function of branch water potential.